The magma-assisted removal of Arabia in Afar: Evidence from dike injection in the Ethiopian rift captured using InSAR and seismicity

Derek Keir,[1,2] Carolina Pagli,[1] Ian D. Bastow,[3] and Atalay Ayele[4]

[1]   In seismically and tectonically active regions, the present-day strain field tends to bias interpretation of the geological record. This is usually reasonable, but in areas such as triple junctions, the orientation of stress and the locus of strain can evolve abruptly in space and time. We present deformation measurements using satellite radar interferometry (InSAR) and seismicity that together capture the intrusion of a ~6 km long, ~1.5 m wide dike into the upper crust of the Ethiopian rift in southern Afar during May 2000. Dike-induced volcano-tectonic seismicity suggests that the intrusion was injected laterally during a period of ~4 days. Seismic moment release accounts for only 5% of the total 1.6×10^{18} Nm geodetic moment, showing that diking accommodates the majority of strain. The intrusion intriguingly strikes at N122°E, perpendicular to the trend of the present-day East African rift. The geometry and age constraints on faulting and volcanic activity in southern Afar, combined with plate reconstructions, suggest that the dike likely intrudes an ~ESE-SE striking magmatic system that localized strain during Oligo-Miocene rifting in the Red Sea and Gulf of Aden. We also identify the southerly extent of the Arabian Plate in Afar during the Oligocene in mantle seismic tomographic images: an abrupt increase in seismic velocity in southern Afar is coincident with a stepped increase of ~20 Myr in the time elapsed since the onset of plate stretching. The anomalous orientation of the May 2000 intrusion implies that African-Arabian tectonics still influences the stress field in southern Afar and is at least partly accommodated by magma intrusion. **Citation:** Keir, D., C. Pagli, I. D. Bastow, and A. Ayele (2011), The magma-assisted removal of Arabia in Afar: Evidence from dike injection in the Ethiopian rift captured using InSAR and seismicity, *Tectonics*, *30*, TC2008, doi:10.1029/2010TC002785.

1. Introduction

[2]   Active tectonics and the present-day strain field that characterize a region often dominate interpretation of the geological record. However, in some areas such as triple junctions, the tectonic processes acting in a region can evolve dramatically over very short length and time scales. One such example is the seismically and volcanically active Afar triangle [*Barberi and Varet*, 1977; *Hofstetter and Beyth*, 2003; *Ayele et al.*, 2007], which exposes subaerially the meeting of the Arabian, Somalian and Nubian Plates in the Horn of Africa [e.g., *McKenzie et al.*, 1970; *Beyene and Abdelsalam*, 2005] (Figure 1). The tectonic evolution of southern Afar has frequently been synthesized in light of the present-day ~ESE-WNW extensional strain field associated with the Miocene-recent Main Ethiopian rift (MER) that bisects the region [e.g., *Kendall et al.*, 2005, 2006; *Rooney et al.*, 2007; *Keranen and Klemperer*, 2008]. However, structural geology constrained with geochronology shows that during the period ~30–10 Ma, southern Afar rifted as a result of the ~NE directed removal of the Arabian plate from Africa [e.g., *Mohr*, 1972; *Tesfaye et al.*, 2003; *Wolfenden et al.*, 2004, 2005; *Ayalew et al.*, 2006; *Bosworth et al.*, 2005] leading to the opening of the Gulf of Aden [e.g., *Leroy et al.*, 2010a, 2010b]. This implies that a near-90° rotation in the direction of extension has occurred in southern Afar during triple junction development, with an associated dramatic reorganization in rate, mechanism and locus of strain.

[3]   Here we use crustal deformation data measured by satellite radar interferometry (InSAR) and seismicity to constrain the geometry and time scale of a dike intrusion into the MER in southern Afar during May 2000 (Figures 2 and 3). The vertical intrusion is ~6 km long and emplaced laterally into the crust at a depth range of 6–12 km over a period of ~4 days. However, the dike has an anomalous strike of ~N122°E which is inconsistent with extension across the MER. We interpret our measurements using a combination of surface morphology, the geological record, alongside insights from the upper mantle seismic velocity structure of the region to show that southern Afar retains a signature of Red Sea–Gulf of Aden tectonics and with it, clues as to the origins of Arabia.

2. Tectonics

[4]   The Miocene-recent Main Ethiopian rift (MER) constitutes the northern part of the East African rift (EAR) system and forms the youngest arm of the rift-rift-rift triple junction currently positioned in central Afar [e.g., *Tesfaye*

---

[1]School of Earth and Environment, University of Leeds, Leeds, UK.
[2]Now at National Oceanography Centre, University of Southampton, Southampton, UK.
[3]Department of Earth Sciences, University of Bristol, Bristol, UK.
[4]Institute of Geophysics, Space Science, and Astronomy, Addis Ababa University, Addis Ababa, Ethiopia.

et al., 2003; *Wolfenden et al.*, 2004] (Figure 1). Since the Quaternary, extensional strain in the MER has localized to ~30 km wide, ~60 km long en echelon magmatic segments encapsulating NNE striking faults and volcanic cones aligned along a rift axis striking perpendicular to the ~N100°E extension direction (Figure 1) [e.g., *Mohr*, 1967; *Hayward and Ebinger*, 1996; *Bilham et al.*, 1999; *Ebinger and Casey*, 2001; *Casey et al.*, 2006; *Corti*, 2008, 2009]. Anomalously fast seismic velocities in the crust beneath these Quaternary axial segments [e.g., *Keranen et al.*, 2004; *Mackenzie et al.*, 2005; *Maguire et al.*, 2006; *Daly et al.*, 2008], coinci-

dent with positive Bouguer anomalies [*Mahatsente et al.*, 1999; *Tiberi et al.*, 2005; *Cornwell et al.*, 2006] suggest that the localized emplacement of axial mafic intrusions has dominated extension during Quaternary-recent times.

[5] In the central portions of the MER, the Quaternary-recent axial segments right step laterally by ~10–15 km and are set within a ~60 km wide rift valley defined by NE striking Miocene age border faults that likely exploit similarly oriented Proterozoic lithospheric fabric (Figure 1) [e.g., *Gashawbeza et al.*, 2004; *Bonini et al.*, 2005; *Keranen and Klemperer*, 2008; *Agostini et al.*, 2009]. The major phases
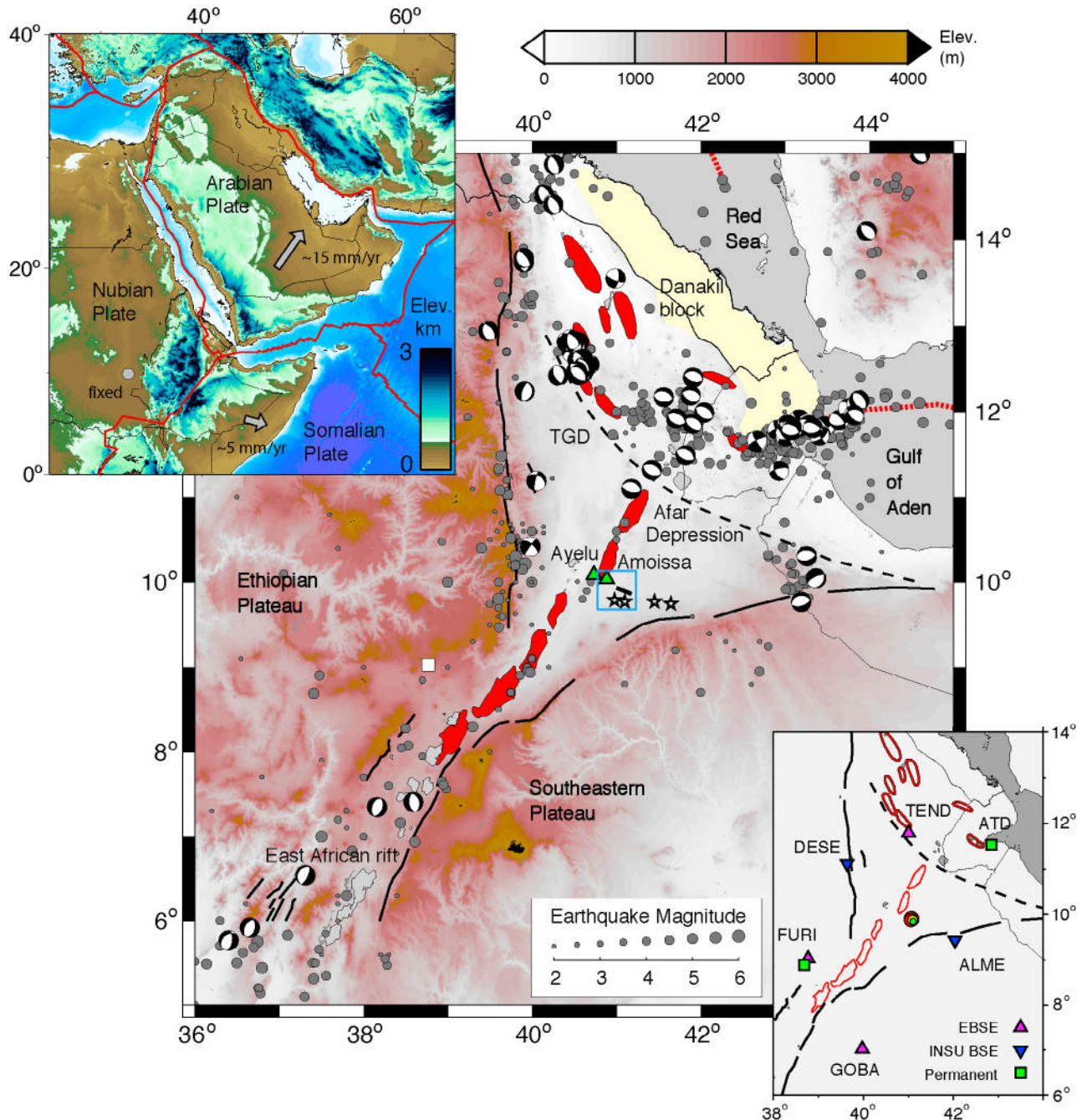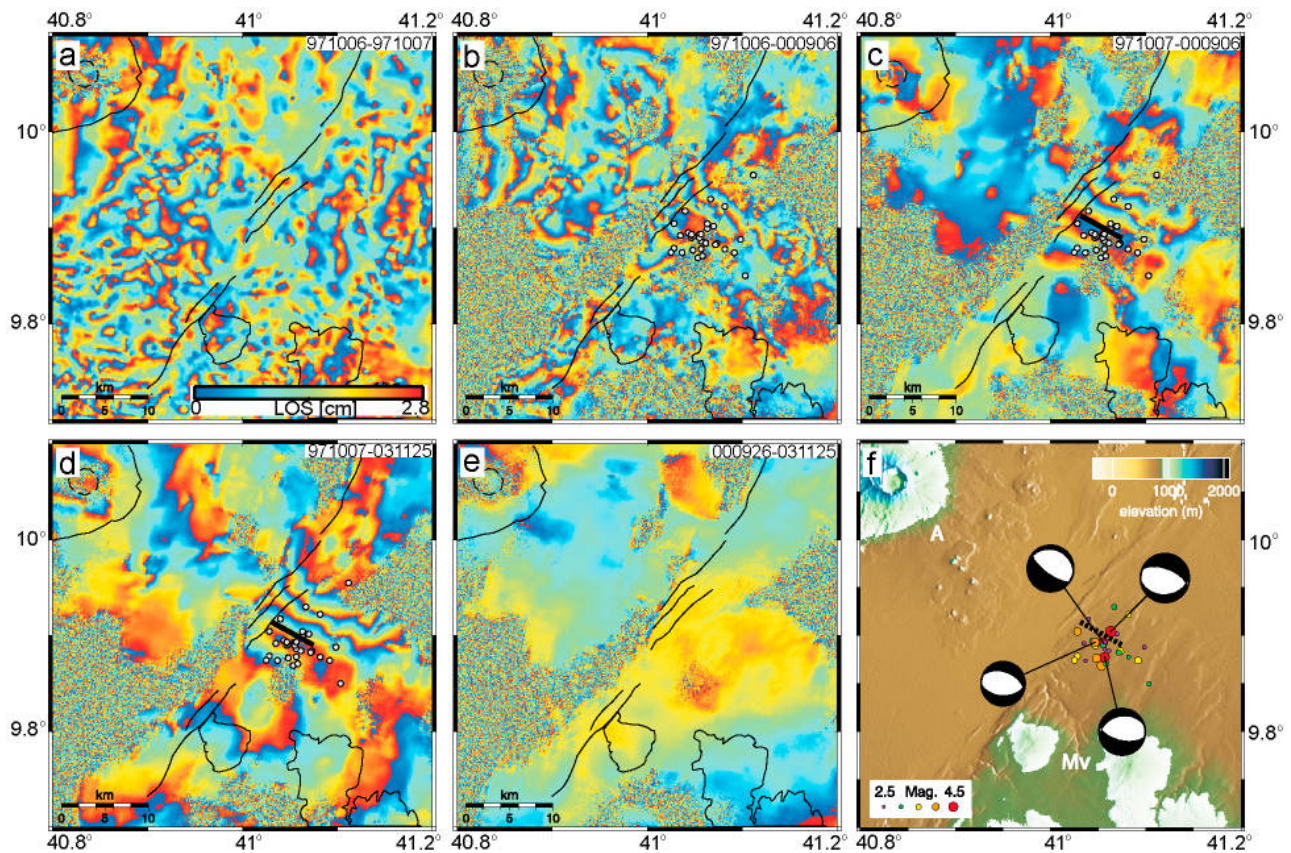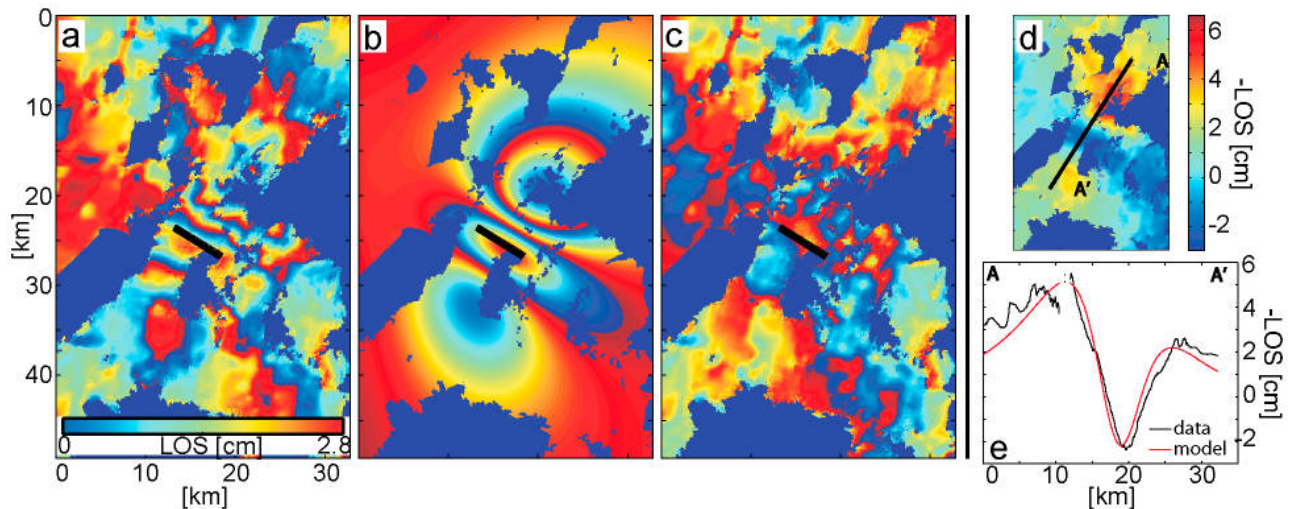

Figure 1

Figure 2. Observed interferograms during 6 October 1997 to 25 November 2003 and seismicity during the May 2000 intrusion. The position of distinctive topographic and tectonic features visible in Figure 2f are traced as black lines on all the interferograms. (a) Prediking interferogram showing no deformation in the region. The time span of the interferogram is marked in the top right corner (YYMMDD) in all panels. Scale bar shows line of sight (LOS) displacement measured in centimeters and is also applicable to all the displayed interferograms. (b–d) Codiking interferograms covering the May 2000 dike intrusion with the locations of the associated cluster plotted as light gray circles. The best fit dike model is shown as a solid black line. (e) Postdiking interferogram showing no deformation. (f) Locations of the dike intrusion, earthquakes, and focal mechanisms during May 2000 plotted on topography. The best fit modeled dike is displayed as a dashed black line. Earthquakes are colored and scaled according to magnitude. Focal mechanisms are from *Ayele et al.* [2006]. A is Amoissa volcano, and Mv is Miocene volcanoes.

Figure 1. Tectonic framework of the Afar depression displayed on topography. Solid black lines show Oligo-Miocene border faults of the Red Sea, Aden, and East African rifts. Red segments show the Quaternary-recent subaerial rift axes. Stars show Late Miocene age (~7 Ma) volcanoes. Green triangles are the Quaternary-recent Ayelu and Amoissa volcanoes (Amoissa is also known in the literature as Aabida, Dabita, and Adwa). Dashed lines show the Tendaho-Goba'ad Discontinuity (TGD). Gray circles show large earthquakes during 1960–2009. The data set during 1960–1997 is sourced from a compilation of global and regional catalogs [*Ayele and Kulhánek*, 1997], and earthquakes during 1997–2009 are from the National Earthquake Information Center (NEIC). Earthquake focal mechanisms are from the Global Centroid Moment Tensor (CMT) catalog. The blue square shows the study region in Figure 2, and the black line within shows the location of the May 2000 intrusion. Top left inset shows topography of NE Africa and Arabia. Gray arrows show plate motions relative to a fixed Nubian plate. Bottom right inset shows location of seismic stations used to locate earthquakes during May 2000. Green squares are the permanent IRIS/USGS station FURI located near Addis Ababa and the Geoscope station ATD in Djibouti. Purple triangles are temporary Ethiopia Broadband Seismic Experiment (EBSE) operated during 2000–2002 [e.g., *Benoit et al.*, 2006], and blue inverted triangles are Institut National des Sciences de l'Univers (INSU) broadband seismic experiment operated during 1999–2002 [e.g., *Sicilia et al.*, 2008].

Figure 3. (a) Interferogram after orbital correction for the May 2000 dike. (b) Best fit model assuming a uniform opening Okada tensile dislocation described in the text. The position of the best fit model dike is shown as a solid black line. (c) Residual interferogram generated by subtracting the model interferograms from the data. (d) Unwrapped interferogram. (e) Profiles of surface deformation across A-A′ showing the data and the model.

of mechanical stretching and thinning of lithosphere beneath the MER and associated growth of border faults in the upper crust is constrained by stratigraphy exposed at the rift margins. South of ~7°N, faulting was well established by ~18 Ma [*WoldeGabriel et al.*, 1990; *Ebinger et al.*, 1993; *Rooney*, 2010]. Between 7°N and 10°N, however, synrift growth of sedimentary and volcanic sequences, as well as fission track thermochronology on exposed basement, indicates rapid growth of border faults started somewhat later, between 6 and 11 Ma [*Ukstins et al.*, 2002; *Wolfenden et al.*, 2004; *Bonini et al.*, 2005; *Abebe et al.*, 2010].

[6] The structure and tectonic history of the Miocene-recent MER south of ~10°N strongly contrasts the north-ernmost ~150 km of the rift, where the Quaternary-recent MER axis strikes ~NNE within the broad Afar Depression (Figure 1). Here, the rift axis is set within mutually perpen-dicular western and southern margins of the Afar depression where rifting initiated at ~30 Ma in the southern Red Sea [e.g., *Wolfenden et al.*, 2005; *Ayalew et al.*, 2006] and at ~35 Ma along the full length of the Gulf of Aden [e.g., *Leroy et al.*, 2010a] (Figure 1). The northernmost MER therefore rifts lithosphere already extended by ~20 Myr of ~NE oriented African-Arabian plate separation prior to for-mation of the MER. This marked change in age since initial lithospheric stretching and faulting in southern Afar is evident in the abrupt 10 km decrease in crustal thickness from 35 km thick in the central MER to ~25 km thick in the northern MER [*Makris and Ginzburg*, 1987; *Dugda et al.*, 2005; *Maguire et al.*, 2006; *Stuart et al.*, 2006; *Cornwell et al.*, 2010]. The northern end of the MER currently terminates at the Tendaho-Goba'ad Discontinuity (TGD) (Figure 1).

[7] Kinematic models constrained by GPS data suggest ~6–8 mm/yr of ~N100°E directed opening in the central and northern MER (Figure 1) [e.g., *Jestin et al.*, 1994; *Fernandes et al.*, 2004; *Stamps et al.*, 2008]. Similar models

suggest ~15 mm/yr of ~N35°E directed opening across the western Gulf of Aden rift [e.g., *Jestin et al.*, 1994]. Current opening across the kinematically complex southern Red Sea rift is well constrained with a relatively high density of GPS measurements [e.g., *ArRajehi et al.*, 2010; *McClusky et al.*, 2010]. These data show that south of ~16°N, the rift bifurcates into two branches: the main Red Sea and the subaerial Red Sea rift in Afar (Danakil Depression) (Figure 1). Partitioning of extension between rift branches varies line-arly along strike; north of ~16°N, ~N50°E oriented exten-sion at ~15 mm/yr is all on the main Red Sea rift while south of ~13°N, extension of ~20 mm/yr has transferred com-pletely into Afar, meaning that the southern portion of the highly extended Danakil block currently has the same plate motion velocity as the Arabian plate [*Vigny et al.*, 2006; *McClusky et al.*, 2010]. The present-day tectonics of northern Afar suggests that the Danakil block is likely to form a minor continental block on the future Arabian passive margin [*Eagles et al.*, 2002; *Peron-Pinvidic and Manatschal*, 2010], a structure perhaps analogous to the Rockall Bank on the eastern margin of the North Atlantic [see, e.g., *White et al.*, 2008].

[8] Rifting in Ethiopia currently occurs above a broad, slow seismic velocity anomaly in the mantle [e.g., *Ritsema and van Heijst*, 2000; *Benoit et al.*, 2006; *Bastow et al.*, 2008, 2011; *Sicilia et al.*, 2008]. This has been interpreted as a region of anomalously high temperature and partial melt that are primarily caused by the combined effects of the African superswell and ongoing MER extensional tectonics [e.g., *Bastow et al.*, 2010].

3. Data and Methods

[9] In May 2000, a notable cluster of seismic activity occurred in a region <25 km^2 near Ayelu and Amoissa

volcanoes in southern Afar (Figures 1 and 2) and was detected by seismograph stations operating in the region [*Ayele et al.*, 2006]. Here, we probe the sequence in space and time by analyzing the deformation field with InSAR and through detailed analysis of the evolution in seismicity.

3.1. InSAR Observations

[10] An interferogram can be regarded as a map of deformation, where each cycle of colors (fringe) represents a ground displacement in the line of sight (LOS) to the satellite of ~2.8 cm, if using ERS data. We formed a series of five interferograms covering the Ayelu-Amoissa volcanic complex, using radar images acquired by the ERS1/2 satellites between 1997 and 2003 (Figure 2). We used images from Track 6 in descending orbit, as this was the only Track where images were collected over the time span of the dike intrusion. The interferograms span different time periods allowing us to separate prediking, codiking and postdiking deformation (Figure 2). The codiking interferograms (Figures 2b–2d) show a consistent deformation signal, arranged in three lobes. The same deformation pattern is observed in at least two interferograms formed using completely independent pairs, indicating that the signal is real and not caused by atmospheric disturbances. About one fringe of positive LOS displacement (ground moving away from the satellite) is centered at the location of the seismic swarm in May 2000 and two lobes of negative LOS displacement (ground moving toward the satellite) are observed on the sides. The pattern is consistent with dike emplacement at depth, causing subsidence immediately above the dike and uplift and horizontal movement away from the dike on the opposite sides of the dike plane (Figure 3). The deformation pattern is asymmetric due to the satellite viewing geometry. Up to two fringes of negative LOS displacement are observed on the northeastern lobe, as both the horizontal and vertical displacements are toward the satellite. While in the southwestern lobe only one fringe is observed, as the negative LOS displacement from the flank uplift tends to be canceled by the positive LOS displacement from the horizontal displacement. Therefore we conclude that this deformation signal is real and related to the seismic activity in May 2000. Prediking and postdiking interferograms show no significant deformation.

3.2. Seismicity

[11] We use seismicity data recorded during May 2000 in southern Afar (Figure 1) by the 1999–2002 INSU (Institut National des Sciences de l'Univers) broadband seismic experiment [e.g., *Montagner et al.*, 2007], and the 2000–2002 Ethiopian Broadband Seismic Experiment (EBSE) [e.g., *Brazier et al.*, 2008] (Figure 1). Data were also sourced from two permanent stations: FURI (IRIS/USGS) and ATD (GEOSCOPE) (Figure 1). The seven seismic stations are 150–400 km from the earthquake hypocenters and provide a maximum azimuthal gap in station coverage of 70°. To minimize the influence of phase reading errors and a variable station distribution on earthquake locations, we relocate 32 earthquakes with the clearest P and S wave arrivals at all seismic stations. Earthquakes are located using

a 1-D seismic velocity model constrained by the results of wide-angle seismic experiments [*Makris and Ginzburg*, 1987; *Maguire et al.*, 2006]. Due to the large distance between earthquakes and stations we fix hypocenter depths to 7 km, consistent with best fit source depths determined using waveform modeling of the four largest magnitude earthquakes [*Ayele et al.*, 2006]. These earthquake depths are also consistent with estimates of effective elastic thickness of the Afar lithosphere [*Ebinger and Hayward*, 1996; *Pérez-Gussinyé et al.*, 2009]. Our resultant locations have estimated horizontal errors of <3 km.
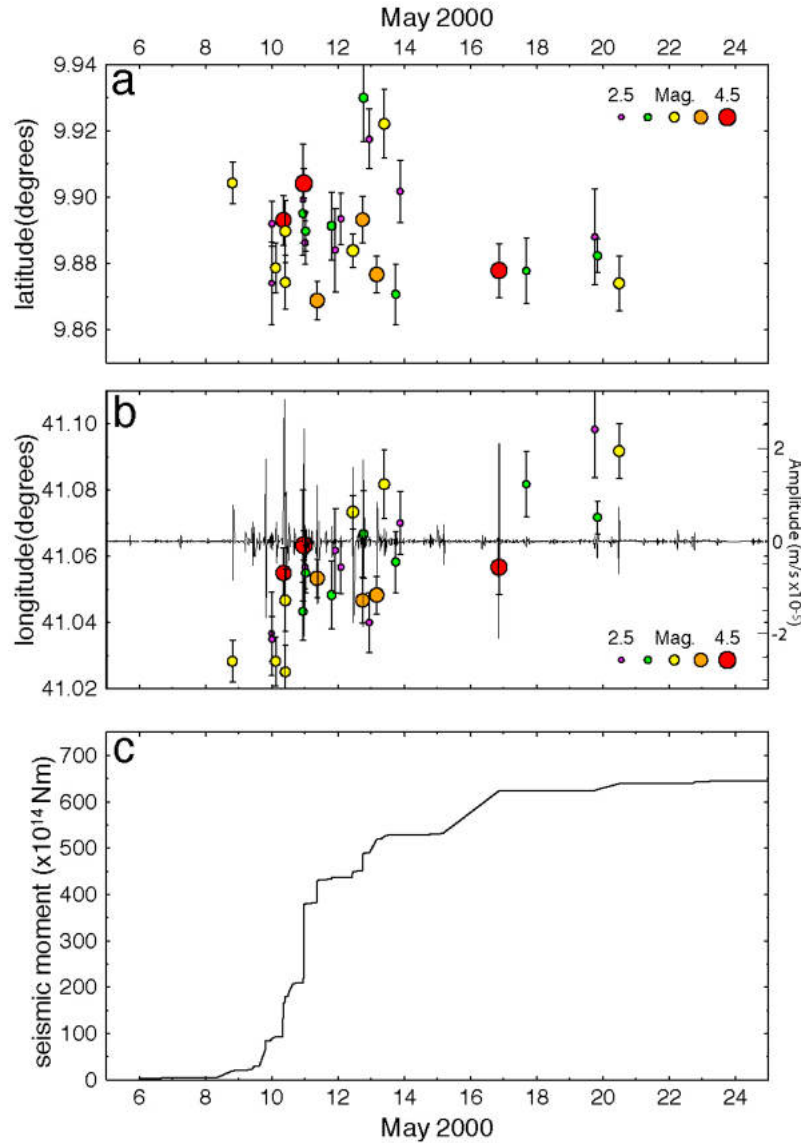
[12] To constrain the release of seismic energy, we expand the data set to ~150 earthquakes that were detected on at least three seismic stations. Local magnitudes (M_L) of these earthquakes were computed, with maximum zero-to-peak amplitude measured on simulated horizontal component Wood-Anderson displacement seismograms after removal of instrument response [*Richter*, 1935]. These measurements are used in conjunction with hypocentral distances to estimate local magnitude (M_L) using the distance correction applicable to the MER [*Keir et al.*, 2006]. These analyses also show that all the $M_L > 3.5$ earthquakes have been included in the data set of 32 relocated events, and are therefore the major contributors to the total seismic strain. Seismic moment release (M_o) is determined using empirical relationships between M_L, m_b, and M_o [e.g., *Kanamori*, 1977; *Hanks and Kanamori*, 1979; *Scordilis*, 2006]. Earthquake source parameters and moment magnitudes for the four largest earthquakes are determined by moment tensor inversion on three-component displacement waveforms, with a full description of methods provided by *Ayele et al.* [2006].

4. Results

4.1. InSAR Modeling

[13] To explain the deformation pattern we use a dike injection at the location of the seismic swarm in May 2000. The deformation source is buried in a uniform elastic isotropic half-space, with a Poisson's ratio of 0.25. The interferogram in Figure 2c was selected for the modeling as it covers the shortest codiking interval and it shows good coherence and low level of atmospheric disturbances. We found the ten best fit model parameters using a nonlinear inversion, employing a simulated annealing search [e.g., *Cervelli et al.*, 2001; *Pagli et al.*, 2007]. Before performing the inversion, the interferogram was cleaned from orbital contributions by subtracting a linear tilt. The data were then unwrapped (Figure 3d) and quadtree partitioned in order to transform the interferometric deformation from a series of fringes to a continuous scale and to reduce the data size [e.g., *Jonsson et al.*, 2002].

[14] We found a best fit solution (Figure 3) consisting of a 6.1 km long dyke, dipping 86°NE, extending from 6 to 12 km depth, striking N122°E and with 1.5 m of uniform opening. The model gives an RMS misfit of 7.8 mm and a reduced χ^2 of 0.6. The reduced χ^2 equals $r^T \sum^{-1} \frac{r}{n-m}$, where r is the residual, $\sum$ is the data covariance matrix, n is the number of data points and m is the number of model parameters. The reduced χ^2 is expected to be 1 if the optimal solution is found and our assumption of data errors (10 mm)

Figure 4. Evolution of seismic deformation during May 2000. (a) Epicenter latitude against time shows no discernible pattern. (b) Epicenter longitude against time shows that seismicity migrates ~8 km east after the start of intense seismic activity. The graph is plotted above the continuous vertical component velocity seismogram. (c) Cumulative seismic moment release during the earthquake cluster. The rate of seismic moment release is markedly higher during lateral migration of earthquakes.

is correct. Therefore a χ^2 of 0.6 indicates that the fit of the model and a 10 mm uncertainty for the interferometric data are reasonable. Geodetic moment for the best fit model is ~1.6×10^{18} Nm, assuming a shear modulus of 30 GPa.

4.2. Seismicity

[15] Earthquake epicenters define an ~8 km long, ~3 km wide, ~N120°E striking elongate cluster located ~40 km ESE of the Ayelu-Amoissa volcanic complex (Figure 2). Seismicity is spatially coincident with surface subsidence measured using InSAR (Figure 3). Moment tensor inversion shows normal slip on ESE-WNW to E-W striking faults, and a best fit source depth of 7 km (Figure 2).

[16] Within the cluster, the location of earthquakes migrates through time (Figure 4). During 1–7 May, infrequent and low-magnitude earthquakes (M_L < 2.5) are located at the western side of the cluster. However, during 10–13 May, both the number and magnitude of earthquakes show significant increase (Figure 4). This approximately 4 day phase of relatively rapid seismic moment release is also characterized by a progressive ~8 km eastward migration of seismicity. The cluster of earthquakes shows no discernible N-S migration with time (Figure 4). After 14 May,

seismicity decreased and is localized to the eastern portion of the deformed zone. The total seismic moment release during the earthquake cluster is ~6.5 × 10^{16} Nm, ~4% of the total 1.6 × 10^{18} Nm strain estimated from the geodetic data, showing that the majority of deformation is accommodated elastically by the intrusion.

[17] During 10–13 May 2000, the peak in seismic moment release and synchronous lateral migration of high-frequency volcanic-tectonic earthquakes is consistent with a model of seismicity induced by locally concentrated extensional stress near the leading edge of a laterally propagating dike [e.g., *Rubin and Gillard*, 1998; *Roman and Cashman*, 2006]. Assuming the migrating seismicity tracks the lateral growth of the intrusion, we estimate that the dike propagated ~8 km eastward over 4 days at an average velocity of ~2 km/d. However, closer inspection of the temporal pattern of seismicity suggests the dike grew rapidly to half its final length of ~4 km on 10 May 2000, after which lateral dike growth slowed progressively (Figure 4).

5. Discussion

[18] In the following sections we place constraints on the magmatic plumbing system that gave rise to the May 2000 event. In doing so, we show how a clear understanding of Ethiopia's asynchronous rift sector development is of paramount importance when interpreting present-day tectonic activity.

5.1. Magma Plumbing System Associated With the May 2000 Intrusion

[19] Combined measurements of deformation using InSAR and seismicity provide strong evidence that strain during the May 2000 event is accommodated principally by lateral intrusion of a vertical dike. Such observations of deformation during dike intrusion are rare, with the only previous example from the East African rift being the similarly scaled July–August 2007 intrusion beneath the Ngorongoro–Ol Doinyo Lengai–Gelai chain of volcanoes in the Natron rift, Tanzania [e.g., *Baer et al.*, 2008; *Calais et al.*, 2008; *Biggs et al.*, 2009].

[20] The May 2000 intrusion in the MER is subparallel to the ~ESE striking Ayelu-Amoissa chain of aligned volcanic centers that dominate the morphology of the right stepping MER offset at ~10°N (Figures 3 and 5). At the surface, both Ayelu and Amoissa are characterized by rhyolitic flows, with minor basaltic cones and lava fields occupying the eastern periphery of the volcanic center [*Chernet et al.*, 1998]. InSAR data show no evidence of significant surface deformation at either volcano, indicating that magmatic movements at shallow levels did not occur. However, the west-to-east migration of seismicity suggests strongly that magma is sourced from a reservoir beneath the volcanic center. The lack of measureable subsidence at the surface above the magma source is likely due to deflation of a relatively deep magma reservoir, making detection of associated surface subsidence difficult. Alternatively, the reservoir may not have deflated despite evacuation of magma into the new dike. Such lack of reservoir deflation can be caused by expansion of magma in the chamber due to gasses exsolving

in response to pressure drop, or from the presence of stiff spherical magma chamber that does not easily deform [e.g., *Rivalta and Segall*, 2008].

[21] While our observations of deformation do not constrain the precise location or depth of the magma reservoir that feeds the dike, geophysical and geochemical data from similar Quaternary-recent silicic volcanic centers in Ethiopia support residence of partial melt in upper crustal plumbing systems beneath central volcanoes. Quaternary-recent volcanic rocks of the MER are predominantly rhyolites and ignimbrites sourced from axial calderas [e.g., *Boccaletti et al.*, 1999], with the chemistry of these felsic rocks indicating partial fractionation from basalts in shallow crustal reservoirs [e.g., *Peccerillo et al.*, 2003, 2007; *Rooney et al.*, 2007, 2011]. The presence of a magma reservoir in the upper crust beneath the Ayelu-Amoissa volcanic chain is also supported by the presence of a particularly slow seismic velocity anomaly imaged beneath these volcanoes using tomographic inversion of surface waves with a period of 5–10 s, which are sensitive to seismic structures in the depth range ~5–10 km [*Guidarelli et al.*, 2009].
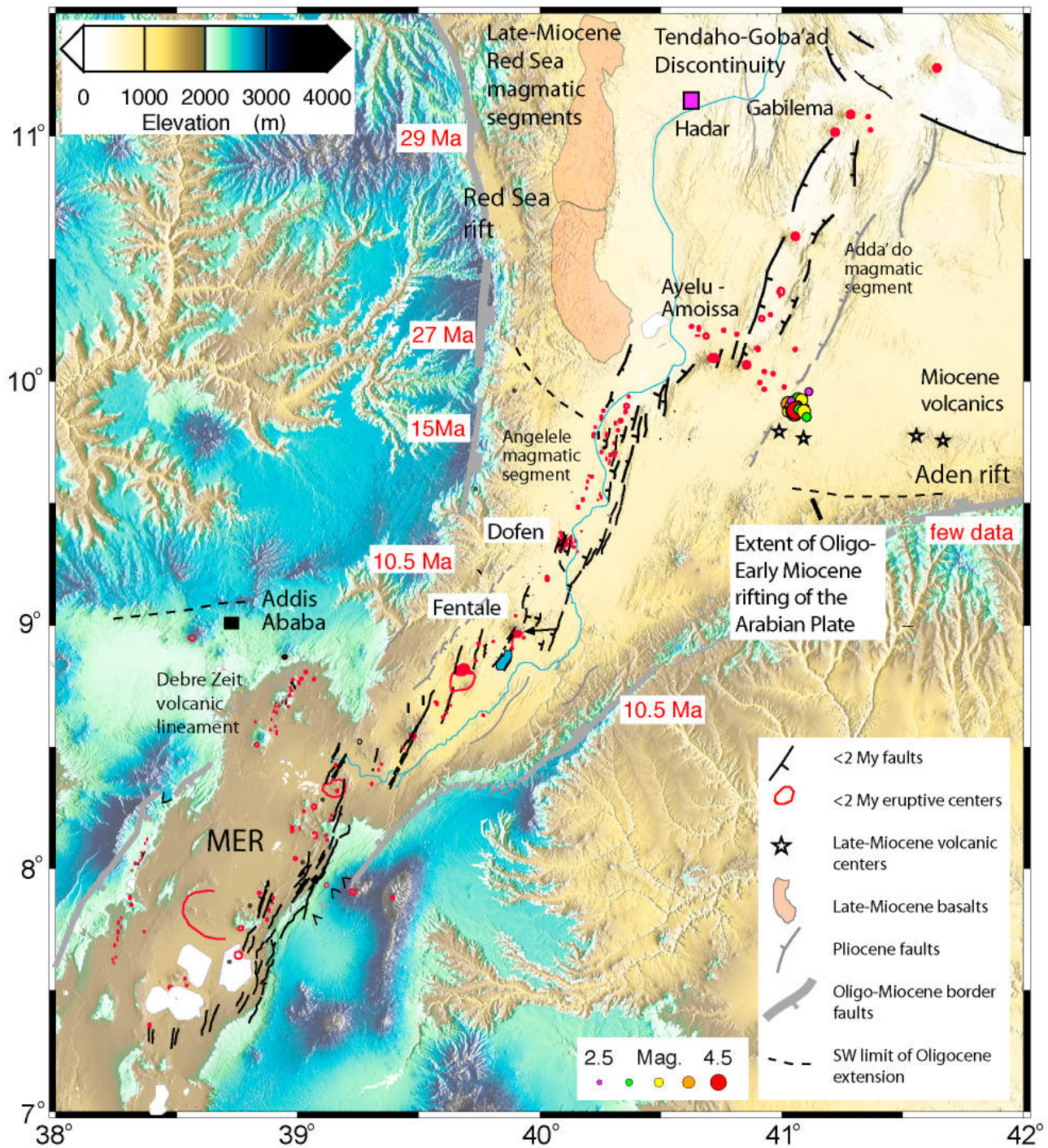
[22] The May 2000 intrusion in the MER was not associated with extrusive volcanic activity. Nevertheless, the spatial arrangement of nearby basaltic cones at the eastern periphery of the Quaternary volcanic field suggests that the intrusion has a relatively primitive composition. This is consistent with relatively lower-viscosity and higher-density magma being required for lateral transport to larger distances away from a magma reservoir located beneath a volcanic edifice [e.g., *Pinel and Jaupart*, 2004], which is expressed at many volcanic fields by more primitive eruptive products around the edges of more evolved, silicic central volcanoes [e.g., *Hildreth*, 1981; *Gudmundsson*, 1995; *Ebinger and Casey*, 2001], and as observed in the Ayelu-Amoissa volcanic system.

[23] The geophysical and geological evidence presented here in support of lateral dike intrusion bears similarities to the style of deformation during the 1975–84 Krafla rifting episode in the North Volcanic Zone, Iceland, as well as to the ongoing Dabbahu rifting episode in northern Afar. In these regions, combined seismicity and geodetic data sets provide strong evidence that mafic dikes are predominantly intruded laterally into the crust, with the basaltic magma sourced via middle to upper crustal magma reservoirs located beneath volcanic centers [e.g., *Brandsdóttir and Einarsson*, 1979; *Einarsson and Brandsdóttir*, 1980; *Buck et al.*, 2006; *Ayele et al.*, 2009; *Keir et al.*, 2009b; *Ebinger et al.*, 2010; *Grandin et al.*, 2010]. These results suggest that dike intrusion at divergent plate boundaries generally propagate laterally from a central reservoir, rather than emplaced vertically from the mantle.

5.2. Implications for the Evolution of the Afar Triple Junction

[24] Dike intrusions usually strike perpendicular to the direction of minimum compressive stress [e.g., *McKenzie et al.*, 1992; *Rubin*, 1995]. However, the N122°E oriented May 2000 intrusion approximately parallels the ~N100°E oriented regional extension across the MER [e.g., *Bendick*

Figure 5. Simplified structural map of the Main Ethiopian rift (modified after *Casey et al.* [2006]). Thick gray lines are border faults with the annotated dates showing the age of the onset of rifting estimated from Ar^{40}/Ar^{39} dates on synrift volcanic rocks [*Ukstins et al.*, 2002; *Wolfenden et al.*, 2004, 2005; *Ayalew et al.*, 2006]. Thin gray lines are Pliocene age faults, and thin black lines are Quaternary-recent faults along the rift axis. Red shapes show major Quaternary to recent volcanic centers. The light red shaded region is Late Miocene basalt flows (~7–8 Ma) [*Wolfenden et al.*, 2004], and stars show Late Miocene volcanic centers (~7 Ma) on the southern margin of Afar [*Chernet et al.*, 1998]. Earthquake epicenters of the May 2000 cluster are plotted with color and size scaled to local magnitude (M$_L$).

et al., 2006; *Stamps et al.*, 2008] and therefore accommodates little Nubian-Somalian Plate separation.

[25] The geometry of the modeled dike relative to the Ayelu-Amoissa volcanic chain suggests that the intrusion strikes radially away from the volcanic center (Figure 3). Both load of volcanic edifice and pressurization in a subsurface magma reservoir generates radial maximum horizontal stress [e.g., *Acocella and Neri*, 2009] and therefore provides a plausible mechanism to locally overprint regional stresses from Nubian-Somalian plate separation. However, aligned volcanic cones are restricted to the western flank of Ayelu volcano and the eastern flank of Amoissa, with the implication that loading and magma pressurization effects do not dominate the longer-term strain field. The dike also strikes approximately ~SE, intriguingly perpendicular to the present-day ~NE oriented African-Arabian extension direction that characterized southern Afar prior to ~10 Ma. In the subsequent paragraphs we cite geological and geophysical evidence that magmatic processes in southern Afar, exemplified by the May 2000 event, remain strongly influenced by a long history of Arabian tectonics.

[26] Spatial and temporal constraints on the evolution of southern Afar come from structural mapping and dating of synrift volcanic rocks along the western Afar margin. These studies show that during Oligocene to Upper Miocene times (~7–8 Ma) active extension and volcanism in the southern Red Sea rift characterized the western margin of Afar as far south as ~10°N [*Wolfenden et al.*, 2005; *Ayalew et al.*, 2006] (Figure 5). The now inactive ~ESE-SE striking faults and aligned chains of volcanoes near the southern margin of the Afar depression provide indelible evidence of the ~NE oriented African-Arabian Oligocene-Miocene strain field [e.g., *Chernet et al.*, 1998; *Tesfaye et al.*, 2003]. Zones of localized extension and volcanism accommodating ~NE motion of the Arabian Plate have, since ~10 Ma, migrated northeastward by ~150 km from southern Afar to their current position NE of the TGD [e.g., *Tesfaye et al.*, 2003; *Audin et al.*, 2004], coeval with the ~NE migration of the ~E-W oriented strain field of the northernmost MER [e.g., *Mohr*, 1972; *Wolfenden et al.*, 2004]. The Ayelu-Amoissa volcanic chain is thus located near the southwestern extent of ~NE-SW directed Oligo-Miocene rifting and strikes perpendicular to the strain field that characterized it.
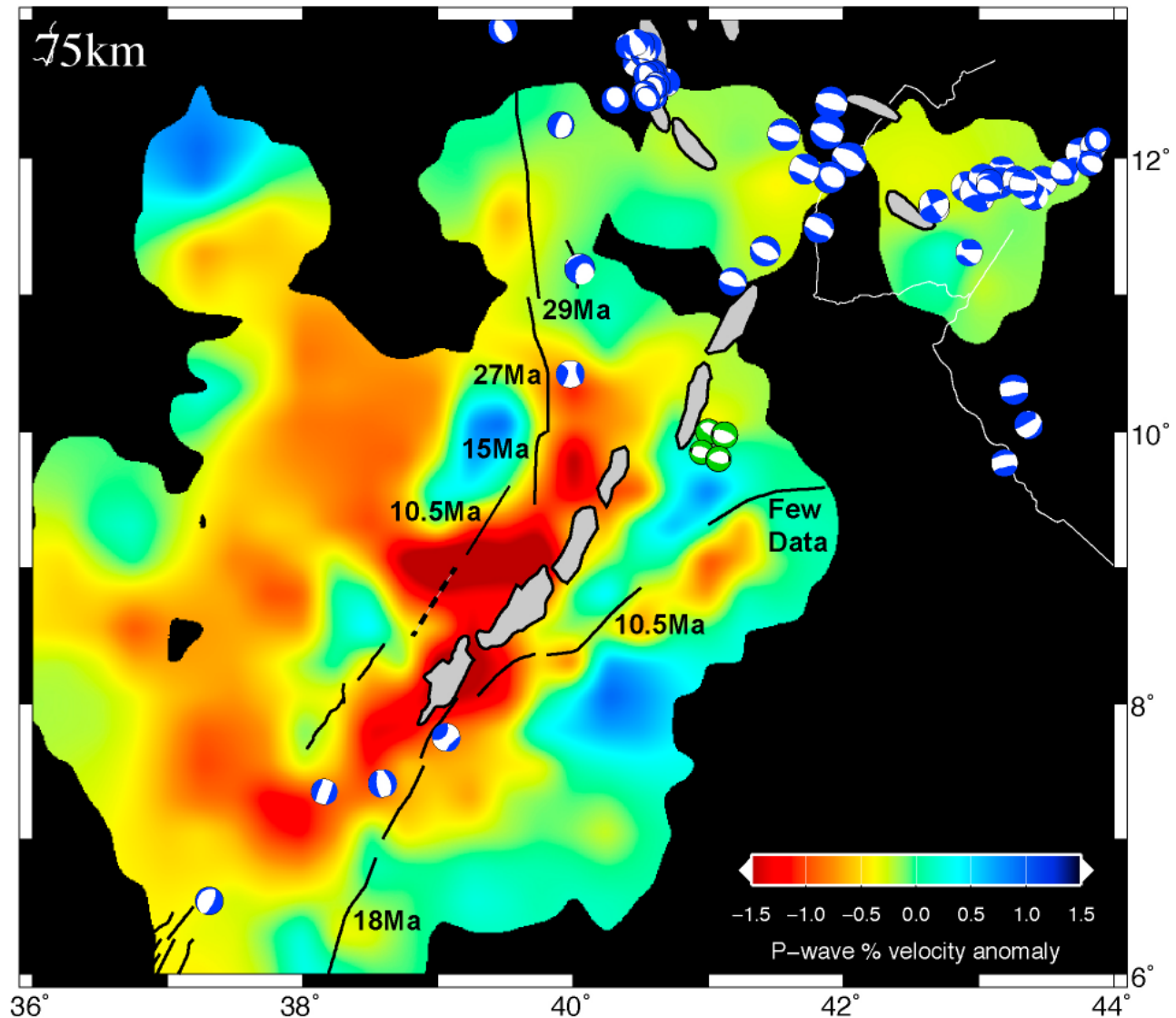
[27] The asynchronous development of rifting in Ethiopia has marked implications for the current thermal conditions and generation of melt. The increase in rift age of ~20 Myr north of 10°N, where the Miocene-recent MER connects with the Oligocene-recent Red Sea and Gulf of Aden rifts shows up remarkably clearly in seismic tomographic images of upper mantle velocity structure [*Bastow et al.*, 2008] (Figure 6). The extreme low velocities observed in the MER between 7°N and 10°N are well explained by a rifting model in which plate stretching at ~6–10 Ma generated decompression melts in the underlying asthenosphere. The short period of time since stretching and faulting were replaced by magma intrusion as the dominant mechanism of strain means that these mantle thermal anomalies have barely had chance to cool by conduction to the surface [*Bastow et al.*, 2010]. In contrast, further north in southern Afar where

rifting began ~20 Myr earlier, cooling of the decompressed asthenosphere by conduction through the overlying plate to the surface, and progressive removal of lower melting point constituents by magma intrusion during progressive rifting explains why present-day uppermost mantle velocities are slightly higher than in the MER between 7°N and 10°N [*Bastow et al.*, 2008, 2010]. In support of the tomographic observations, studies of seismic anisotropy indicate a peak in melt volume in the 7°N–10°N sector of the MER [e.g., *Kendall et al.*, 2005; *Bastow et al.*, 2010].

[28] The greater time available for conductive cooling of the mantle as the MER merges into the Afar depression explains the lack of Quaternary-recent rift flank volcanism along the Oligo-Miocene age southern and southwestern margins of Afar. Magma supply is maintained in the Ayelu-Amoissa system, however, due to its coincidence with focused supply of ongoing decompression melting beneath the ~30 km wide rift axis of the MER. The paucity of Quaternary-recent rift flank volcanism in Afar contrasts the younger MER south of 10°N where the less than 10 Myr since decompression melting from initial plate stretching provides a ready supply of melt to linear volcanic chains located on rift border faults (e.g., Debre Zeit Volcanic Lineament [e.g., *Rooney et al.*, 2007; *Keir et al.*, 2009a]).

[29] While geophysical monitoring of deformation in Afar suggests that the majority of current extensional strain related to the ~NE motion of the Arabian Plate is accommodated NE of the TGD [e.g., *Wright et al.*, 2006; *Ayele et al.*, 2009; *Hamling et al.*, 2009; *Keir et al.*, 2009b; *Ebinger et al.*, 2010; *McClusky et al.*, 2010], our new observations of ~N35°E directed dike opening in the MER suggest that the motion of Arabia still influences current deformation in southern Afar, where African-Arabian extension began ~30–35 Ma [e.g., *Autin et al.*, 2010; *Leroy et al.*, 2010a, 2010b]. Since dike injection accommodates strain at lower stresses than faulting [e.g., *Bialas et al.*, 2010], the coincidence of ongoing and localized decompression melting beneath the narrow MER axis with favorably oriented magmatic systems formed during the earlier removal of Arabia aids the maintenance of limited ~NE directed extension in the northernmost MER. Further evidence for ongoing African-Arabian deformation being accommodated in southern Afar is provided by moment tensors of large earthquakes occurring since 1960, which shows other earthquakes located near the northern MER axis with ~NE oriented T axes (Figure 6).

[30] Alternatively, the location and orientation of the May 2000 intrusion may be caused by migration of magma along preexisting transverse faults that cut across the northern MER. Structural and volcanology studies in the MER show examples of rift-perpendicular alignment and elongation of QR volcanic centers that correlate to mapped ~ESE-WNW striking faults present near the rift borders. These structures are proposed to influence the initiation and evolution of Quaternary-recent magma chambers and faults along the axis of the MER [e.g., *Mohr*, 1968; *Acocella et al.*, 2003; *Korme et al.*, 2004]. While such ~ESE-WNW striking faults that cut across the MER plausibly formed during the Oligo-Miocene rifting of the Arabian plate from Africa, a pre-Oligocene origin to such structures cannot be ruled out.

Figure 6. Slice at 75 km depth through the P wave relative arrival time tomographic model of Ethiopia by *Bastow et al.* [2008], plotted with the lower hemisphere projection of earthquake focal mechanisms. Blue focal mechanisms are sourced from the CMT catalog. Green focal mechanisms have been computed using moment tensor inversion of data from local stations [*Ayele et al.*, 2006]. Solid black lines indicate border faults. Quaternary-recent magmatic segments are shaded in gray. The annotated dates show the estimated age for the onset of rifting [*Ukstins et al.*, 2002; *Wolfenden et al.*, 2004, 2005; *Ayalew et al.*, 2006]. Note that the lowest seismic velocities in the upper mantle are beneath the MER between 7°N and 10°N, where the geological record suggests initial stretching of the lithosphere and rapid growth of faults in the upper crust occurred during 6–11 Ma. In contrast, further north in central Afar where rifting began ~30–35 Ma, cooling of the decompressed asthenosphere by conduction through the plate to the surface, and progressive removal of lower melting point constituents by magma intrusion during progressive rifting explains why present-day uppermost mantle velocities are higher. Present-day active tectonics in southern Afar can thus be used to map the ~NE migration of the Afar triple junction and, by inference, the relatively rapid northeast motion of the Arabian plate.

[31] Our multidisciplinary study demonstrates the likely importance that the motion of the Arabian plate has on the tectonic evolution of the whole of the Afar depression, including the southern portion that is now within the MER. We show that ~NE oriented strain in Afar related to the separation of Arabia is currently not only restricted to the current incipient Red Sea and Gulf of Aden plate boundaries such as the Dabbahu magmatic segment [e.g., *Wright et al.*, 2006], Tendaho Graben [*Acocella*, 2010], and Asal-Ghoubbet rift [e.g., *Doubre and Peltzer*, 2007; *Doubre et al.*, 2007],

and invites future detailed GPS studies to better understand the distributed strain field at an evolving subaerial triple junction. A detailed appreciation of the changes in the orientation, rate and locus of strain throughout rift evolution is also paramount for constraining both subsidence and thermal histories of sedimentary basins throughout the region. Since these factors exert a major control on the elevation and shape of the land surface, they also strongly influence the evolution of paleoclimate and paleogeography [e.g., *Kalb*, 1995; *Redfield et al.*, 2003]. In addition, the geological history of major anthropological sites in southwestern Afar such as Hadar have been shaped by both Red Sea and MER extension (Figure 5), meaning that unraveling the spatial and temporal evolution of the strain field also has direct relevance to understanding patterns of early human speciation.

ern Afar suggest that the dike intrudes an ~ESE-SE trending volcanic system formed during the separation of the Arabian Plate from Africa during Oligo-Miocene times. Such zones of localized ~NE directed extension have since been largely overprinted by development of the northernmost East African rift. Our interpretation is supported by the abrupt northward, along-rift increase in seismic velocity of the upper mantle in southern Afar coincident with a stepped increase in age since the major phases of initial mechanical stretching of the plate. The observed seismic and magmatic activity in SW Afar indicates that a NE-oriented strain field still influences the MER, showing a component of strain from the current ~NE motion of the Arabian Plate is distributed away from the incipient Red Sea and Gulf of Aden plate boundaries in northern and eastern Afar.

6. Conclusions

[32] We have used InSAR and seismicity that record the intrusion of a dike into the upper crust of the Ethiopian rift in southern Afar during May 2000. Elastic models of InSAR data show that the dike is ~6 km long, ~1.5 m wide, and strikes N122°E, an intriguing orientation since it is subparallel to the current regional extension direction of the MER. The geological record and tectonic history of south-

References

Abebe, T., M. L. Balestrieri, and G. Bigazzi (2010), The central Main Ethiopian rift is younger than 8 Ma: Confirmation through apatite fission-track thermochronology, *Terra Nova*, *22*, 470–476, doi:10.1111/j.1365-3121.2010.00968.

Acocella, V. (2010), Coupling volcanism and tectonics along divergent plate boundaries: Collapsed rifts from central Afar, Ethiopia, *Geol. Soc. Am. Bull.*, *122*, 1717–1728, doi:10.1130/B30105.1.

Acocella, V., and M. Neri (2009), Dike propagation in volcanic edifices: Overview and possible developments, *Tectonophysics*, *471*, 67–77, doi:10.1016/j.tecto.2008.10.002.

Acocella, V., T. Korme, F. Salvini, and R. Funiciello (2003), Elliptic calderas in the Ethiopian rift: Control of pre-existing structures, *J. Volcanol. Geotherm. Res.*, *119*, 189–203, doi:10.1016/S0377-0273(02)00342-6.

Agostini, A., G. Corti, A. Zeoli, and G. Mulugeta (2009), Evolution, pattern, and partitioning of deformation during oblique continental rifting: Inferences from lithospheric-scale centrifuge models, *Geochem. Geophys. Geosyst.*, *10*, Q11015, doi:10.1029/2009GC002676.

ArRajehi, A., et al. (2010), Geodetic constraints on present-day motion of the Arabian Plate: Implications for Red Sea and Gulf of Aden rifting, *Tectonics*, *29*, TC3011, doi:10.1029/2009TC002482.

Audin, L., X. Quidelleur, E. Coulié, V. Courtillot, S. Gilder, I. Manighetti, P.-Y. Gillot, P. Tapponnier, and T. Kidane (2004), Palaeomagnetism and K-Ar and ⁴⁰Ar/³⁹Ar ages in the Ali Sabieh area (Republic of Djibouti and Ethiopia): Constraints on the mechanism of Aden ridge propagation into southeastern Afar during the last 10 Myr, *Geophys. J. Int.*, *158*, 327–345, doi:10.1111/j.1365-246X.2004.02286.x.

Autin, J., S. Leroy, M. O. Beslier, E. d'Acremont, P. Razin, A. Ribodetti, N. Bellahsen, C. Robin, and K. Al Toubi (2010), Continental break-up history of a deep magma-poor margin based on seismic reflection data (northeastern Gulf of Aden margin, offshore Oman), *Geophys. J. Int.*, *180*, 501–519, doi:10.1111/j.1365-246X.2009.04424.x.

Ayalew, D., C. Ebinger, E. Bourdon, E. Wolfenden, G. Yirgu, and N. Grassineau (2006), Temporal compositional variation of syn-rift rhyolites along the western margin of the southern Red Sea and northern Main Ethiopian rift, *Geol. Soc. Spec. Publ.*, *259*, 121–130, doi:10.1144/GSL.SP.2006.259.01.10.

Ayele, A., and O. Kulhánek (1997), Spatial and temporal variations of seismicity in the Horn of Africa from 1960 to 1993, *Geophys. J. Int.*, *130*, 805–810, doi:10.1111/j.1365-246X.1997.tb01875.x.

Ayele, A., A. A. Nyblade, C. A. Langston, M. Cara, and J.-J. Lévêque (2006), New evidence for Afro-Arabian plate separation in southern Afar, *Geol. Soc. Spec. Publ.*, *259*, 133–141, doi:10.1144/GSL.SP.2006.259.01.12.

Ayele, A., G. Stuart, I. Bastow, and D. Keir (2007), The August 2002 earthquake sequence in north Afar: Insights into the neotectonics of the Danakil microplate, *J. Afr. Earth Sci.*, *48*, 70–79, doi:10.1016/j.jafrearsci.2006.06.011.

Ayele, A., D. Keir, C. Ebinger, T. J. Wright, G. W. Stuart, W. R. Buck, E. Jacques, G. Ogubazghi, and J. Sholan (2009), September 2005 mega-dike emplacement in the Manda-Harraro nascent oceanic rift (Afar Depression), *Geophys. Res. Lett.*, *36*, L20306, doi:10.1029/2009GL039605.

Baer, G., Y. Hamiel, G. Shamir, and R. Nof (2008), Evolution of a magma-driven earthquake swarm and triggering of the nearby Oldoinyo Lengai eruption, as resolved by InSAR, ground observations, and elastic modeling, East African rift, 2007, *Earth Planet. Sci. Lett.*, *272*, 339–352, doi:10.1016/j.epsl.2008.04.052.

Barberi, F., and J. Varet (1977), Volcanism of Afar: Small-scale plate tectonics implications, *Geol. Soc. Am. Bull.*, *88*, 1251–1266, doi:10.1130/0016-7606(1977)88<1251:VOASPT>2.0.CO;2.

Bastow, I. D., A. A. Nyblade, G. W. Stuart, T. O. Rooney, and M. H. Benoit (2008), Upper mantle seismic structure beneath the Ethiopian hot spot: Rifting at the edge of the African low-velocity anomaly, *Geochem. Geophys. Geosyst.*, *9*, Q12022, doi:10.1029/2008GC002107.

Bastow, I. D., S. Pilidou, J.-M. Kendall, and G. W. Stuart (2010), Melt-induced seismic anisotropy and magma assisted rifting in Ethiopia: Evidence from surface waves, *Geochem. Geophys. Geosyst.*, *11*, Q0AB05, doi:10.1029/2010GC003036.

Bastow, I. D., D. Keir, and E. Daly (2011), The Ethiopian Afar Geoscientific Lithospheric Experiment (EAGLE): Probing the transition from continental rifting to sea-floor spreading, *Spec. Pap. Geol. Soc. Am.*, in press.

Bendick, R., S. McClusky, R. Bilham, L. Asfaw, and S. Klemperer (2006), Distributed Nubia-Somalia relative motion and dike intrusion in the Main Ethiopian rift, *Geophys. J. Int.*, *165*, 303–310, doi:10.1111/j.1365-246X.2006.02904.x.

Benoit, M. H., A. A. Nyblade, and J. C. VanDecar (2006), Upper mantle P wave speed variations beneath Ethiopia and the origin of the Afar hotspot, *Geology*, *34*, 329–332, doi:10.1130/G22281.1.

Beyene, A., and M. G. Abdelsalam (2005), Tectonics of the Afar Depression: A review and synthesis, *J. Afr. Earth Sci.*, *41*, 41–59, doi:10.1016/j.jafrearsci.2005.03.003.

Bialas, R. W., W. R. Buck, and R. Qin (2010), How much magma is required to rift a continent?, *Earth Planet. Sci. Lett.*, *292*, 68–78, doi:10.1016/j.epsl.2010.01.021.

Biggs, J., F. Amelung, N. Gourmelen, T. H. Dixon, and S. W. Kim (2009), InSAR observations of 2007 Tanzania rifting episode reveal mixed fault and dyke extension in an immature continental rift, *Geophys. J. Int.*, *179*, 549–558, doi:10.1111/j.1365-246X.2009.04262.x.

Bilham, R., R. Bendick, K. Larson, P. Mohr, J. Braun, S. Tesfaye, and L. Asfaw (1999), Secular and tidal strain across the Main Ethiopian rift, *Geophys. Res. Lett.*, *26*(18), 2789–2792, doi:10.1029/1998GL005315.

Boccaletti, M., R. Mazzuoli, M. Bonini, T. Trua, and B. Abebe (1999), Plio-Quaternary volcanic activity in the northern sector of the Main Ethiopian rift (MER): Relationships with oblique rifting, *J. Afr. Earth Sci.*, *29*, 679–698, doi:10.1016/S0899-5362(99)00124-4.

Bonini, M., G. Corti, F. Innocenti, P. Manetti, F. Mazzarini, T. Abebe, and Z. Pecskay (2005), Evolution of the Main Ethiopian rift in the frame

of Afar and Kenya rift propagation, *Tectonics*, *24*, TC1007, doi:10.1029/2004TC001680.

Bosworth, W., P. Huchon, and K. McClay (2005), The Red Sea and Gulf of Aden basins, *J. Afr. Earth Sci.*, *43*, 334–378, doi:10.1016/j.jafrearsci.2005.07.020.

Brandsdóttir, B., and P. Einarsson (1979), Seismic activity associated with the September 1977 deflation of the Krafla central volcano in northeastern Iceland, *J. Volcanol. Geotherm. Res.*, *6*, 197–212, doi:10.1016/0377-0273(79)90001-5.

Brazier, R. A., Q. Miao, A. A. Nyblade, A. Ayele, and C. A. Langston (2008), Local magnitude scale for the Ethiopian Plateau, *Bull. Seismol. Soc. Am.*, *98*, 2341–2348, doi:10.1785/0120070266.

Buck, W. R., P. Einarsson, and B. Brandsdóttir (2006), Tectonic stress and magma chamber size as controls on dike propagation: Constraints from the 1975–1984 Krafla rifting episode, *J. Geophys. Res.*, *111*, B12404, doi:10.1029/2005JB003879.

Calais, E., et al. (2008), Strain accommodation by slow slip and dyking in a youthful continental rift, East Africa, *Nature*, *456*, 783–787, doi:10.1038/nature07478.

Casey, M., C. Ebinger, D. Keir, R. Gloaguen, and F. Mohammed (2006), Strain accommodation in transitional rifts: Extension by magma intrusion and faulting in Ethiopian rift magmatic segments, *Geol. Soc. Spec. Publ.*, *259*, 143–163, doi:10.1144/GSL.SP.2006.259.01.13.

Cervelli, P., M. H. Murray, P. Segall, Y. Aoki, and T. Kato (2001), Estimating source parameters from deformation data, with an application to the March 1997 earthquake swarm off Izu Peninsula, Japan, *J. Geophys. Res.*, *106*, 11,217–11,237, doi:10.1029/2000JB900399.

Chernet, T., W. K. Hart, J. L. Aronson, and R. C. Walter (1998), New age constraints on the timing of volcanism and tectonism in the northern Main Ethiopian rift–southern Afar transition zone (Ethiopia), *J. Volcanol. Geotherm. Res.*, *80*, 267–280, doi:10.1016/S0377-0273(97)00035-8.

Cornwell, D. G., G. D. Mackenzie, R. W. England, P. K. H. Maguire, L. M. Asfaw, and B. Oluma (2006), Northern Main Ethiopian rift crustal structure from new high-precision gravity data, *Geol. Soc. Spec. Publ.*, *259*, 307–321, doi:10.1144/GSL.SP.2006.259.01.23.

Cornwell, D. G., P. K. H. Maguire, R. W. England, and G. W. Stuart (2010), Imaging detailed crustal structure and magmatic intrusion across the Ethiopian rift using a dense linear broadband array, *Geochem. Geophys. Geosyst.*, *11*, Q0AB03, doi:10.1029/2009GC002637.

Corti, G. (2008), Control of rift obliquity on the evolution and segmentation of the main Ethiopian rift, *Nat. Geosci.*, *1*, 258–262, doi:10.1038/ngeo160.

Corti, G. (2009), Continental rift evolution: From rift initiation to incipient break-up in the Main Ethiopian rift, East Africa, *Earth Sci. Rev.*, *96*, 1–53, doi:10.1016/j.earscirev.2009.06.005.

Daly, E., D. Keir, C. J. Ebinger, G. W. Stuart, I. D. Bastow, and A. Ayele (2008), Crustal tomographic imaging of a transitional continental rift: The Ethiopian rift, *Geophys. J. Int.*, *172*, 1033–1048, doi:10.1111/j.1365-246X.2007.03682.x.

Doubre, C., and G. Peltzer (2007), Fluid-controlled faulting process in the Asal rift, Djibouti, from 8 yr of radar interferometry observations, *Geology*, *35*, 69–72, doi:10.1130/G23022A.1.

Doubre, C., I. Manighetti, L. Dorbath, C. Dorbath, D. Bertil, and J. C. Delmond (2007), Crustal structure and magmato-tectonic processes in an active rift (Asal-Ghoubbet, Afar, East Africa): 2. Insights from the 23-year recording of seismicity since the last rifting event, *J. Geophys. Res.*, *112*, B05406, doi:10.1029/2006JB004333.

Dugda, M. T., A. A. Nyblade, J. Julia, C. A. Langston, C. J. Ammon, and S. Simiyu (2005), Crustal structure in Ethiopia and Kenya from receiver function analysis: Implications for rift development in eastern Africa, *J. Geophys. Res.*, *110*, B01303, doi:10.1029/2004JB003065.

Eagles, G., R. Gloaguen, and C. Ebinger (2002), Kinematics of the Danakil microplate, *Earth Planet. Sci. Lett.*, *6398*, 1–14.

Ebinger, C. J., and M. Casey (2001), Continental breakup in magmatic provinces: An Ethiopian example, *Geology*, *29*, 527–530, doi:10.1130/0091-7613(2001)029<0527:CBIMPA>2.0.CO;2.

Ebinger, C. J., and N. J. Hayward (1996), Soft plates and hot spots: Views from Afar, *J. Geophys. Res.*, *101*, 21,859–21,876, doi:10.1029/96JB02118.

Ebinger, C. J., T. Yemane, G. WoldeGabriel, J. Aronson, and R. Walter (1993), Eocene-recent volcanism and faulting in the southern Main Ethiopian rift, *J. Geol. Soc.*, *150*, 99–108, doi:10.1144/gsjgs.150.1.0099.

Ebinger, C., A. Ayele, D. Keir, J. Rowland, G. Yirgu, T. Wright, M. Belachew, and I. Hamling (2010), Length and timescales of rift faulting and magma intrusion: The Afar rifting cycle from 2005 to present, *Annu. Rev. Earth Planet. Sci.*, *38*, 439–466, doi:10.1146/annurev-earth-040809-152333.

Einarsson, P., and B. Brandsdóttir (1980), Seismological evidence for lateral magma intrusion during the July 1978 deflation of the Krafla volcano in NE Iceland, *J. Geophys.*, *47*, 160–165.

Fernandes, R. M. S., B. A. C. Ambrosius, R. Noomen, L. Bastos, L. Combrinck, J. M. Miranda, and W. Spakman (2004), Angular velocities of Nubia and Somalia from continuous GPS data: Implications on present-day relative kinematics, *Earth Planet. Sci. Lett.*, *222*, 197–208, doi:10.1016/j.epsl.2004.02.008.

Gashawbeza, E. M., S. L. Klemperer, A. A. Nyblade, K. T. Walker, and K. M. Keranen (2004), Shear-wave splitting in Ethiopia: Precambrian mantle anisotropy locally modified by Neogene rifting, *Geophys. Res. Lett.*, *31*, L18602, doi:10.1029/2004GL020471.

Grandin, R., A. Socquet, E. Jacques, N. Mazzoni, J.-B. de Chabalier, and G. C. P. King (2010), Sequence of rifting in Afar, Manda-Hararo rift, Ethiopia, 2005–2009: Time-space evolution and interactions between dikes from interferometric synthetic aperture radar and static stress change modeling, *J. Geophys. Res.*, *115*, B10413, doi:10.1029/2009JB000815.

Gudmundsson, A. (1995), Infrastructure and mechanics of volcanic systems in Iceland, *J. Volcanol. Geotherm. Res.*, *64*, 1–22, doi:10.1016/0377-0273(95)92782-Q.

Guidarelli, M., G. W. Stuart, J. O. S. Hammond, J.-M. Kendall, and C. J. Ebinger (2009), Crustal structure across Afar, Ethiopia, from surface wave tomography, *Eos Trans. AGU*, *90*(52), Fall Meet. Suppl., Abstract T31B-1809.

Hamling, I. J., A. Ayele, L. Bennati, E. Calais, C. J. Ebinger, D. Keir, E. Lewi, T. J. Wright, and G. Yirgu (2009), Geodetic observations of the ongoing Dabbahu rifting episode: New dyke intrusions in 2006 and 2007, *Geophys. J. Int.*, *178*, 989–1003, doi:10.1111/j.1365-246X.2009.04163.x.

Hanks, T. C., and H. Kanamori (1979), A moment magnitude scale, *J. Geophys. Res.*, *84*, 2348–2350, doi:10.1029/JB084iB05p02348.

Hayward, N. J., and C. J. Ebinger (1996), Variations in the along-axis segmentation of the Afar rift system, *Tectonics*, *15*, 244–257, doi:10.1029/95TC02292.

Hildreth, W. (1981), Gradients in silicic magma chambers: Implications for lithospheric magmatism, *J. Geophys. Res.*, *86*, 10,153–10,192, doi:10.1029/JB086iB11p10153.

Hofstetter, R., and M. Beyth (2003), The Afar Depression: Interpretation of the 1960–2000 earthquakes, *Geophys. J. Int.*, *155*, 715–732, doi:10.1046/j.1365-246X.2003.02080.x.

Jestin, F., P. Huchon, and J. M. Gaulier (1994), The Somalia plate and the East African rift system: Present-day kinematics, *Geophys. J. Int.*, *116*, 637–654, doi:10.1111/j.1365-246X.1994.tb03286.x.

Jonsson, S., H. Zebker, P. Segall, and F. Amelung (2002), Fault slip distribution of the 1999 Mw 7.2 Hector mine earthquake, California, estimated from satellite radar and GPS measurements, *Bull. Seismol. Soc. Am.*, *92*, 1377–1389, doi:10.1785/0120000922.

Kalb, J. E. (1995), Fossil elephantoids, Awash paleo-lake basins, and the Afar triple junction, Ethiopia, *Palaeogeogr. Palaeoclimatol. Palaeoecol.*, *114*, 357–368, doi:10.1016/0031-0182(94)00088-P.

Kanamori, H. (1977), The energy release in great earthquakes, *J. Geophys. Res.*, *82*, 2981–2987, doi:10.1029/JB082i020p02981.

Keir, D., G. W. Stuart, A. Jackson, and A. Ayele (2006), Local earthquake magnitude scale and seismicity rate for the Ethiopian rift, *Bull. Seismol. Soc. Am.*, *96*, 2221–2230, doi:10.1785/0120060051.

Keir, D., I. D. Bastow, K. A. Whaler, E. Daly, D. G. Cornwell, and S. Hautot (2009a), Lower crustal earthquakes near the Ethiopian rift induced by magmatic processes, *Geochem. Geophys. Geosyst.*, *10*, Q0AB02, doi:10.1029/2009GC002382.

Keir, D., et al. (2009b), Evidence for focused magmatic accretion at segment centers from lateral dike injections captured beneath the Red Sea rift in Afar, *Geology*, *37*, 59–62, doi:10.1130/G25147A.1.

Kendall, J.-M., G. W. Stuart, C. J. Ebinger, I. D. Bastow, and D. Keir (2005), Magma-assisted rifting in Ethiopia, *Nature*, *433*, 146–148, doi:10.1038/nature03161.

Kendall, J.-M., S. Pilidou, D. Keir, I. D. Bastow, G. W. Stuart, and A. Ayele (2006), Mantle upwellings, melt migration and the rifting of Africa: Insights from seismic anisotropy, *Geol. Soc. Spec. Publ.*, *259*, 55–72, doi:10.1144/GSL.SP.2006.259.01.06.

Keranen, K., and S. L. Klemperer (2008), Discontinuous and diachronous evolution of the Main Ethiopian rift: Implications for development of continental rifts, *Earth Planet. Sci. Lett.*, *265*, 96–111, doi:10.1016/j.epsl.2007.09.038.

Keranen, K., S. L. Klemperer, R. Gloaguen, and EAGLE Working Group (2004), Three-dimensional seismic imaging of a protoridge axis in the Main Ethiopian rift, *Geology*, *32*, 949–952, doi:10.1130/G20737.1.

Korme, T., V. Acocella, and B. Abebe (2004), The role of pre-existing structures in the origin, propagation and architecture of faults in the Main Ethiopian rift, *Gondwana Res.*, *7*, 467–479, doi:10.1016/S1342-937X(05)70798-X.

Leroy, S., E. d'Acremont, C. Tiberi, C. Basuyau, F. Lucazeau, and H. Sloan (2010a), Recent off-axis volcanism in the eastern Gulf of Aden: Implications for plume-ridge interaction, *Earth Planet. Sci. Lett.*, *293*, 140–153, doi:10.1016/j.epsl.2010.02.036.

Leroy, S., et al. (2010b), Contrasting styles of rifting in the eastern Gulf of Aden: A combined wide-angle, multichannel seismic, and heat flow survey, *Geochem. Geophys. Geosyst.*, *11*, Q07004, doi:10.1029/2009GC002963.

Mackenzie, G. D., H. Thybo, and P. K. H. Maguire (2005), Crustal velocity structure across the Main Ethiopian rift: Results from two-dimensional wide-angle seismic modelling, *Geophys. J. Int.*, *162*, 994–1006, doi:10.1111/j.1365-246X.2005.02710.x.

Maguire, P. K. H., et al. (2006), Crustal structure of the northern Main Ethiopian rift from the EAGLE controlled-source survey: A snapshot of incipient lithospheric break-up, *Geol. Soc. Spec. Publ.*, *259*, 269–292, doi:10.1144/GSL.SP.2006.259.01.21.

Mahatsente, R., G. Jentzsch, and T. Jahr (1999), Crustal structure of the Main Ethiopian rift from gravity data: 3-dimensional modeling, *Tectonophysics*, *313*, 363–382, doi:10.1016/S0040-1951(99)00213-9.

Makris, J., and A. Ginzburg (1987), The Afar Depression: Transition between continental rifting and sea-floor spreading, *Tectonophysics*, *141*, 199–214, doi:10.1016/0040-1951(87)90186-7.

McClusky, S., et al. (2010), Kinematics of the southern Red Sea–Afar Triple Junction and implications for plate dynamics, *Geophys. Res. Lett.*, *37*, L05301, doi:10.1029/2009GL041127.

McKenzie, D. P., D. Davies, and P. Molnar (1970), Plate tectonics of Red Sea and East Africa, *Nature*, *226*, 243–248, doi:10.1038/226243a0.

McKenzie, D., J. M. McKenzie, and R. S. Saunders (1992), Dike emplacement on Venus and on Earth,

J. Geophys. Res., *97*, 15,977–15,990, doi:10.1029/92JE01559.

Mohr, P. A. (1967), Major volcano-tectonic lineament in the Ethiopian rift system, *Nature*, *213*, 664–665, doi:10.1038/213664a0.

Mohr, P. A. (1968), Transcurrent faulting in the Ethiopian rift system, *Nature*, *218*, 938–941, doi:10.1038/218938a0.

Mohr, P. A. (1972), Surface structure and plate tectonics of Afar, *Tectonophysics*, *15*, 3–18, doi:10.1016/0040-1951(72)90045-5.

Montagner, J.-P., B. Marty, E. Stutzmann, D. Sicilia, M. Cara, R. Pik, J.-J. Lévêque, G. Roult, E. Beucler, and E. Debayle (2007), Mantle upwellings and convective instabilities revealed by seismic tomography and helium isotope geochemistry beneath eastern Africa, *Geophys. Res. Lett.*, *34*, L21303, doi:10.1029/2007GL031098.

Pagli, C., F. Sigmundsson, R. Pedersen, P. Einarsson, T. Árnadóttir, and K. L. Feigl (2007), Crustal deformation associated with the 1996 Gjáp subglacial eruption, Iceland: InSAR studies in the affected areas adjacent to the Vatnajökull ice cap, *Earth Planet. Sci. Lett.*, *259*, 24–33, doi:10.1016/j.epsl.2007.04.019.

Peccerillo, A., M. R. Barberio, G. Yirgu, D. Ayalew, M. Barbieri, and T. W. Wu (2003), Relationships between mafic and peralkaline silicic magmatism in continental rift settings: A petrological, geochemical and isotope study of the Gedemsa Volcano, central Ethiopian rift, *J. Petrol.*, *44*, 2003–2032, doi:1093/petrology/egg068.

Peccerillo, A., C. Donati, A. P. Santo, A. Orlando, G. Yirgu, and D. Ayalew (2007), Peterogenesis of silicic peralkaline rocks in the Ethiopian rift: Geochemical evidence and volcanological implications, *J. Afr. Earth Sci.*, *48*, 161–173, doi:10.1016/j.jafrearsci.2006.06.010.

Pérez-Gussinyé, M., M. Metois, M. Fernández, J. Vergés, J. Fullea, and A. R. Lowry (2009), Effective elastic thickness of Africa and its relation to other proxies for lithospheric structure and surface tectonics, *Earth Planet. Sci. Lett.*, *287*, 152–167, doi:10.1016/j.epsl.2009.08.004.

Peron-Pinvidic, G., and G. Manatschal (2010), From microcontinents to extensional allochthons: Witnesses of how continents rift and break apart?, *Petrol. Geosci.*, *16*, 189–197, doi:10.1144/1354-079309-903.

Pinel, V., and C. Jaupart (2004), Magma storage and horizontal dyke injection beneath a volcanic edifice, *Earth Planet. Sci. Lett.*, *221*, 245–262, doi:10.1016/S0012-821X(04)00076-7.

Redfield, T. F., W. H. Wheeler, and M. Often (2003), A kinematic model for the development of the Afar Depression and its paleogeographic implications, *Earth Planet. Sci. Lett.*, *216*, 383–398, doi:10.1016/S0012-821X(03)00488-6.

Richter, C. F. (1935), An instrumental earthquake magnitude scale, *Bull. Seismol. Soc. Am.*, *25*, 1–32.

Ritsema, J., and H. van Heijst (2000), New seismic model of the upper mantle beneath Africa, *Geology*, *28*, 63–66, doi:10.1130/0091-7613(2000)28<63:NSMOTU>2.0.CO;2.

Rivalta, E., and P. Segall (2008), Magma compressibility and the missing source for some dike intrusions, *Geophys. Res. Lett.*, *35*, L04306, doi:10.1029/2007GL032521.

Roman, D. C., and K. V. Cashman (2006), The origin of volcano-tectonic earthquake swarms, *Geology*, *34*, 457–460, doi:10.1130/G22269.1.

Rooney, T. O. (2010), Geochemical evidence of lithospheric thinning in the southern Main Ethiopian rift, *Lithos*, *117*, 33–48, doi:10.1016/j.lithos.2010.02.002.

Rooney, T., T. Furman, I. Bastow, D. Ayalew, and G. Yirgu (2007), Lithospheric modification during crustal extension in the Main Ethiopian rift, *J. Geophys. Res.*, *112*, B10201, doi:10.1029/2006JB004916.

Rooney, T. O., I. D. Bastow, and D. Keir (2011), Insights into extensional processes during magma assisted rifting: Evidence from aligned scoria cones, *J. Volcanol. Geotherm. Res.*, doi:10.1016/j.jvolgeores.2010.07.019, in press.

Rubin, A. M. (1995), Propagation of magma-filled cracks, *Annu. Rev. Earth Planet. Sci.*, *23*, 287–336, doi:10.1146/annurev.ea.23.050195.001443.

Rubin, A. M., and D. Gillard (1998), Dike-induced earthquakes: Theoretical considerations, *J. Geophys. Res.*, *103*, 10,017–10,030, doi:10.1029/97JB03514.

Scordilis, E. M. (2006), Empirical global relations converting Ms and mb to moment magnitude, *J. Seismol.*, *10*, 225–236, doi:10.1007/s10950-006-9012-4.

Sicilia, D., et al. (2008), Upper mantle structure of shear-waves velocities and stratification of anisotropy in the Afar hotspot region, *Tectonophysics*, *462*, 164–177, doi:10.1016/j.tecto.2008.02.016.

Stamps, D. S., E. Calais, E. Saria, C. Hartnady, J.-M. Nocquet, C. J. Ebinger, and R. M. Fernandes (2008), A kinematic model for the East African rift, *Geophys. Res. Lett.*, *35*, L05304, doi:10.1029/2007GL032781.

Stuart, G. W., I. D. Bastow, and C. J. Ebinger (2006), Crustal structure of the northern Ethiopian rift from receiver function studies, *Geol. Soc. Spec. Publ.*, *259*, 253–267, doi:10.1144/GSL.SP.2006.259.01.20.

Tesfaye, S., D. J. Harding, and T. M. Kusky (2003), Early continental breakup boundary and migration of the Afar triple junction, Ethiopia, *Geol. Soc. Am. Bull.*, *115*, 1053–1067, doi:10.1130/B25149.1.

Tiberi, C., C. Ebinger, V. Ballu, G. W. Stuart, and B. Oluma (2005), Inverse models of gravity data from the Red Sea–Aden–East African rifts triple junction zone, *Geophys. J. Int.*, *163*, 775–787, doi:10.1111/j.1365-246X.2005.02736.x.

Ukstins, I. A., P. R. Renne, E. Wolfenden, J. Baker, D. Ayalew, and M. Menzies (2002), Matching conjugate volcanic rifted margins: Ar/Ar chronostratigraphy of pre- and syn-rift bimodal flood volcanism in Ethiopia and Yemen, *Earth Planet. Sci. Lett.*, *198*, 289–306, doi:10.1016/S0012-821X(02)00525-3.

Vigny, C., P. Huchon, J.-C. Ruegg, K. Khanbari, and L. M. Asfaw (2006), Confirmation of Arabia plate slow motion by new GPS data in Yemen, *J. Geophys. Res.*, *111*, B02402, doi:10.1029/2004JB003229.

White, R. S., L. K. Smith, A. W. Roberts, P. A. F. Christie, N. J. Kusznir, and the rest of the iSIMM Team (2008), Lower-crustal intrusion on the North Atlantic continental margin, *Nature*, *452*, 460–464, doi:10.1038/nature06687.

WoldeGabriel, G., J. L. Aronson, and R. C. Walter (1990), Geology, geochronology, and rift basin development in the central sector of the Main Ethiopian rift, *Geol. Soc. Am. Bull.*, *102*, 439–458, doi:10.1130/0016-7606(1990)102<0439:GGARBD>2.3.CO;2.

Wolfenden, E., C. Ebinger, G. Yirgu, A. Deino, and D. Ayelew (2004), Evolution of the northern Main Ethiopian rift: Birth of a triple junction, *Earth Planet. Sci. Lett.*, *224*, 213–228, doi:10.1016/j.epsl.2004.04.022.

Wolfenden, E., C. Ebinger, G. Yirgu, P. R. Renne, and S. P. Kelley (2005), Evolution of a volcanic rifted margin: Southern Red Sea, Ethiopia, *Geol. Soc. Am. Bull.*, *117*, 846–864, doi:10.1130/B25516.1.

Wright, T. J., C. J. Ebinger, J. Biggs, A. Ayele, G. Yirgu, D. Keir, and A. Stork (2006), Magma-maintained rift segmentation at continental rupture in the 2005 Afar dyking episode, *Nature*, *442*, 291–294, doi:10.1038/nature04978.

A. Ayele, Institute of Geophysics, Space Science, and Astronomy, Addis Ababa University, PO Box 1176, Addis Ababa, Ethiopia.

I. D. Bastow, Department of Earth Sciences, University of Bristol, Bristol BS8 1RJ, UK.

D. Keir, National Oceanography Centre, University of Southampton, Southampton, SO14 3ZH, UK. (d.keir@soton.ac.uk)

C. Pagli, School of Earth and Environment, University of Leeds, Leeds LS2 9JT, UK.